Universal Scaling of Correlated Diffusion in Colloidal Monolayers

Wei Zhang,[1,2] Na Li,[1] Klemen Bohinc,[3] Penger Tong,[4] and Wei Chen[1,*]

[1]State Key Laboratory of Surface Physics and Department of Physics, Fudan University, Shanghai 200433, China
[2]Department of Physics, Jinan University, Guangzhou 510632, China
[3]Faculty of Health Sciences, University of Ljubljana, Poljanska 26a, Ljubljana 1000, Slovenia
[4]Department of Physics, Hong Kong University of Science and Technology, Clear Water Bay, Kowloon, Hong Kong

(Received 5 November 2012; revised manuscript received 29 June 2013; published 18 October 2013)

Using the techniques of optical microscopy and particle tracking, we measure the correlated diffusion in a monolayer of uniform silica spheres dispersed at a water-air interface. It is found that the correlated motion of the interfacial particles can be well described by two universal response functions, the normalized longitudinal and transverse diffusion coefficients $\tilde{D}_{\parallel}(r/r_0)$ and $\tilde{D}_{\perp}(r/r_0)$, where r is the interparticle distance and $r_0 = a(\lambda_S/a)^{3/2}$ is a new scaling length, which depends on both the Saffman length λ_S and particle radius a. The obtained response functions characterize the crossover behavior of the colloidal monolayers from the subphase-dominated three-dimensional hydrodynamics at low surface coverage to the monolayer-dominated 2D hydrodynamics at high concentrations. The surface viscosity $\eta_s^{(2)}$ of the colloidal monolayer obtained by two-particle rheology compares well with the one-particle measurements.

DOI: 10.1103/PhysRevLett.111.168304 PACS numbers: 82.70.Dd, 05.40.−a, 68.05.Gh, 83.85.Jn

Colloidal monolayers suspended at a liquid-liquid (or liquid-air) interface or near a liquid-solid interface have attracted much attention in recent years; they have served as model systems to study a range of interesting problems of structures and dynamics in two-dimensional soft matter systems [1]. Examples include 2D crystallization [2,3], crystal sublimiation [4], and colloidal glasses [5,6], interactions between similarly charged particles [7–10], and Brownian dynamics at liquid interfaces [11,12]. The colloid-decorated interfaces also have immense practical applications ranging from being used as emulsion stabilizers [13] to colloidosomes [14] and bijels [15]. In addition, colloidal particles have also been used as tracer particles to probe the rheological properties of liquid interfaces coated with a monolayer of surfactant, proteins, or lipids [16–18].

The mobility of the colloidal particles confined to a molecular monolayer at a liquid-air interface is an important quantity that is used to characterize the surface viscosity η_s of the monolayers made of polymers, surfactants, and various biomolecules, such as proteins and lipids [11,16–19]. In two-particle rheology [20,21], one follows the trajectory $\mathbf{s}^i(t)$ of individual particles i as a function of time t and computes the correlated motion between a particle pair i and j via the ensemble averaged tensor product of the particle displacements, $\Delta s_\alpha^i(t,\tau) = s_\alpha^i(t+\tau) - s_\alpha^i(t)$,

$$C_{\alpha\beta}(r,\tau) = \langle \Delta s_\alpha^i(t,\tau) \Delta s_\beta^j(t,\tau) \delta[r - R^{i,j}(t)] \rangle_{i\neq j}, \quad (1)$$

where α and β represent different coordinates, $R^{i,j}$ (and thus r) is the center-to-center distance between the particle pair, τ is the lag time, and the average is taken over distinct particle pairs $i \neq j$ and over time t. In particular, C_{rr} indicates the correlated motion along the line joining the center of the two particles, and $C_{\theta\theta}$ is perpendicular to this line; both are a function of r and τ.

The correlated motion between the particle pairs is affected by the hydrodynamic interactions (HIs) with both the liquid subphase of viscosity η_b and the molecular monolayer having a surface viscosity η_s and thickness h [19,22]. When the Saffman length [23,24] $\lambda_S = \eta_s/\eta_b \gg h$ (large η_s regime), the effect of the liquid subphase is negligibly small and the HIs are essentially 2D [25,26]. In this case, C_{rr} is expected to depend logarithmically on r [23,27]. With deceasing λ_S (or η_s), the effect of the liquid subphase becomes increasingly important and ultimately for small enough λ_S ($\simeq h$), $C_{rr} \sim r^{-1}$ and $C_{\theta\theta} \sim r^{-2}$, as expected for quasi-3D hydrodynamics [18,28,29]. The transition from the subphase-dominated 3D behavior to the membrane-dominated 2D behavior is described by two universal response functions, the normalized longitudinal and transverse diffusion coefficients $\tilde{D}_{\parallel}(r/\lambda_S)$ and $\tilde{D}_{\perp}(r/\lambda_S)$, where λ_S serves as a scaling length and describes at what extent the system can be determined by the 2D hydrodynamics [17,22,30].

Can the continuum hydrodynamic theory for molecular membranes be applied to concentrated colloidal monolayers at the liquid interface, in which the 3D many-body HIs between the particles are involved, but one does not have a theory at the moment to estimate how important they are? Unlike lipid membranes and protein coated liquid interfaces, whose thickness h (1–5 nm) is typically 2–3 orders of magnitude smaller than λ_S (1–10 μm) and they can be treated as a continuum, the colloidal monolayers are not a continuum, the individual spheres feeling a local surface viscosity different from its macroscopic

TABLE I. Silica sphere samples used and their properties obtained from the experiment: particle diameter d, friction coefficients $k^{(0)}$ and $k^{(1)}$, Debye screening length λ_D, maximum area fraction of random packing n_m and intrinsic viscosity $[\eta]$.

Sample: Manufacturer	d (μm)	$k^{(0)}$	$k^{(1)}$	λ_D (μm)	n_m	$[\eta]$
S1: Duke Scientific	1.57 ± 0.06	16.0	0.6	0.4 ± 0.1	0.53	2.1 ± 0.1
S2: Bangs Lab	0.83 ± 0.05	15.2	0.7	0.4 ± 0.1	0.38	2.6 ± 0.1
S3: Duke Scientific	0.73 ± 0.04	16.0	0.6	0.4 ± 0.1	0.33	3.1 ± 0.1

counterpart [31,32], and their film thickness, as measured by the particle radius a, is of the same order as λ_S.

In this Letter, we report a systematic study of the correlated motion in a colloidal monolayer made of uniform silica spheres and dispersed at a water-air interface. It is found that for small lag time τ, the measured $C_{rr}(r, \tau)$ and $C_{\theta\theta}(r, \tau)$ are both linear functions of τ and we obtain the parallel and perpendicular diffusion coefficients, $D_\parallel(r) = C_{rr}/2\tau$ and $D_\perp(r) = C_{\theta\theta}/2\tau$, respectively. The two diffusion coefficients are found to have the universal scaling forms, $\tilde{D}_\parallel(r/r_0)$ and $\tilde{D}_\perp(r/r_0)$, for all samples with different concentrations, where

$$r_0 = a\left(\frac{\lambda_S}{a}\right)^{3/2} \tag{2}$$

is a new scaling length characterizing the crossover behavior of the colloidal monolayers. In the above, $\lambda_S = \eta_s^{(2)}/\eta_b$, with $\eta_s^{(2)}$ being the surface viscosity felt by a pair of particles, as defined in two-particle rheology [17,20].

Three colloidal samples (S1, S2, and S3) of different sizes are used in the experiment. These samples have been carefully characterized previously [33] and their properties are summarized in Table I. The silica spheres are dispersed at the water-air interface following the same procedures as described in [9]. Using the estimated contact angle of 60° [34], we find that approximately 3/4 of the silica particle (by diameter) is immersed in water. The silica spheres are negatively charged and their interaction potential $U(r)$ can be well described by the screened Coulomb potential [33]. The values of the Debye screening length λ_D are given in Table I. The sample cell is viewed under an inverted microscope, and a particle tracking program is used to determine the particle trajectories [35].

Figure 1(a) shows the measured diffusion coefficients $D_\parallel$ and $D_\perp$ as a function of r for sample S1 at different area fractions n occupied by the interfacial particles. In the plot, $D_\parallel$ and $D_\perp$ are normalized by the Stokes-Einstein value $D_0 = k_BT/(6\pi\eta_b a)$, where η_b is the viscosity of water, and r is normalized by d. For small values of n, the measured $D_\parallel$ and $D_\perp$ show some scatter because fewer particles are available in each image for averaging. To further improve the statistics, we averaged the measured $D_\parallel$ and $D_\perp$ over a narrow range of n as indicated by the legends in Fig. 1. The inset shows an example of 26 unaveraged $D_\parallel$'s and $D_\perp$'s in the range $n = 0.03 \pm 0.02$. It is seen from Fig. 1 that the magnitude of $D_\parallel$ and $D_\perp$ increases with n, and they decay with r slower for larger values of n.

Over a finite range of r, the measured $D_\parallel$ and $D_\perp$ can be well described by the power laws: $D_\parallel \propto r^{-\beta_\parallel}$ and $D_\perp \propto r^{-\beta_\perp}$ (not shown). This is an approximate way to describe how fast $D_\parallel$ (and $D_\perp$) decays with r. Figure 1(b) shows the fitted values of $\beta_\parallel$ and $\beta_\perp$ as a function of n for S1. As mentioned above, $D_\parallel$ and $D_\perp$ are expected to depend logarithmically on r for large surface viscosity η_s and become a power-law dependence with $\beta_\parallel = 1$ and $\beta_\perp = 2$, respectively, for small enough η_s [28,29,36,37]. Thus, a smaller $\beta_\parallel$ (or $\beta_\perp$) reflects a larger η_s. In the concentration range $0.03 \lesssim n \lesssim 0.35$, we find the fitted value of $\beta_\parallel$ decreases from 0.89 to 0.67 and $\beta_\perp$ decreases from 1.5 to 1.1, indicating that η_s indeed increases with n. This analysis also suggests that the colloidal monolayer in this

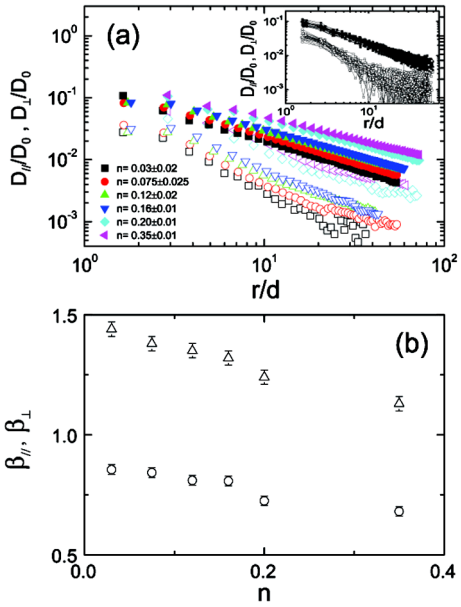

FIG. 1 (color online). (a) Measured $D_\parallel/D_0$ (solid symbols) and $D_\perp/D_0$ (open symbols) as a function of r/d. The measurements are made for S1 at different values of n, which are color coded. Inset shows 26 unaveraged $D_\parallel/D_0$'s and $D_\perp/D_0$'s in the concentration range $n = 0.03 \pm 0.02$ (see text). (b) Fitted values of $\beta_\parallel$ (open circles) and $\beta_\perp$ (open triangles) as a function of area fraction n for S1. The error bars show the standard deviations of the fit.

concentration range is in the crossover regime far from the two limiting cases as discussed above. Similar trends in $D_\parallel$ and $D_\perp$ were also observed for a protein-coated liquid interface [17].

Figure 2(a) shows that all the measured $D_\parallel$ and $D_\perp$ at different n can be superposed onto a single master curve, once $D_\parallel$ (and $D_\perp$) is scaled by a single-particle self-diffusion coefficient $D_s'(n)$ and r is scaled by an adjustable parameter r_0, whose physical meaning will be discussed below. Here $D_s'(n)$ is a directly measured quantity [38] and is linked to the single-particle surface viscosity $\eta_s^{(1)}(n)$ via $D_s'(n) = k_B T/[k^{(1)}\eta_s^{(1)}(n)]$, as defined in one-particle rheology [17,20]. Using this equation, one then obtains $\eta_s^{(1)}(n)$. In the above, $k^{(1)}$ is a known coefficient which only depends on the relative position z/d of the particle at the interface and is independent of n [19]. The values of $k^{(1)}$ are given in Table I.

Once $D_s'(n)$ is determined, r_0 is the only adjustable parameter used to collapse the data for each value of n. In the scaling plots, the measured $D_\parallel$ and $D_\perp$ at large n fall on the left-hand side of the master curves. This is expected because the large-n sample has a higher surface viscosity, which gives rise to a stronger correlation and a weaker r dependence [17,22,30]. It is also found that the obtained master curve for different particle samples can be superposed onto a single curve, once the vertical variable is further normalized by $k^{(1)}$, as shown in Fig. 2(b). In this way, the particle size effect is eliminated [38].

The inset of Fig. 2(b) shows the n dependence of the obtained r_0 for the three colloidal samples. It is found that the scaling length r_0 varies with both n and d. It should be noted that r_0 is determined from the scaling plot only up to a common multiplicative factor Γ. An extra condition is needed to determine the absolute value of Γ (and hence r_0). As shown in Eq. (2), r_0 is directly linked to the two-particle surface viscosity $\eta_s^{(2)}(n)$. We therefore impose a physical constraint on $\eta_s^{(2)}(n)$, namely, $\eta_s^{(2)}(n) = 0$ when $n \to 0$. This condition allows one to have a unique set of r_0 for different values of n, once a relationship between r_0 and $\eta_s^{(2)}$ is determined.

For protein-coated liquid interfaces, the Saffman length $\lambda_S = \eta_s^{(2)}/\eta_b$ was used to scale the measured $D_\parallel(r/\lambda_S)/D_s'(n)$ and $D_\perp(r/\lambda_S)/D_s'(n)$ [17,22,30]. This method of extracting $\eta_s^{(2)}(n)$ from the obtained $\lambda_S(n)$, however, does not work for the colloidal monolayers. As shown in Fig. 1 in [38], the obtained $\eta_s^{(2)}$ is not even a linear function of $\eta_s^{(1)}$; instead, it approximately follows the power law, $\eta_s^{(2)} \sim (\eta_s^{(1)})^{3/2}$. Furthermore, Fig. 2(a) revealed that the obtained $D_\parallel/D_s'(n)$ and $D_\perp/D_s'(n)$ for the colloidal monolayers decay with r slower than the theoretical predictions [17,30].

These observations prompt us to consider a new scaling relation as shown in Eq. (2). Here we have explicitly introduced a particle size dependence in r_0. Figure 3 shows a comparison between $\eta_s^{(2)}$ obtained by using Eq. (2) and $\eta_s^{(1)}$ for the three colloidal samples. In the low concentration regime, we find $\eta_s^{(2)} \simeq \eta_s^{(1)}$. Only at the high-$n$ end ($n = 0.3$), the obtained $\eta_s^{(2)}$ becomes slightly larger than $\eta_s^{(1)}$. In this case, the colloidal monolayer begins to show the heterogeneity (crowding) effect and two-particle rheology gives results different from those obtained by one-particle rheology [17,20]. As expected, Fig. 3 reveals that $\eta_s^{(2)} = \eta_s^{(1)} = 0$ at the $n = 0$ limit.

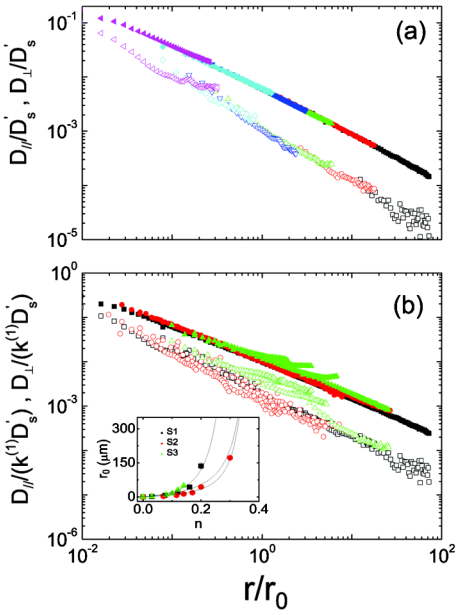

FIG. 2 (color online). (a) Log-log plot of $D_\parallel/D_s'$ (solid symbols) and $D_\perp/D_s'$ (open symbols) as a function of r/r_0 for S1 with different values of n. The data and symbols used are the same as those shown in Fig. 1(a). (b) Log-log plots of $D_\parallel/(k^{(1)}D_s')$ (solid symbols) and $D_\perp/(k^{(1)}D_s')$ (open symbols) as a function of r/r_0 for S1 (black symbols), S2 (red symbols), and S3 (green symbols). Inset shows the n dependence of the obtained r_0 for the three samples. Lines are drawn to guide the eye.

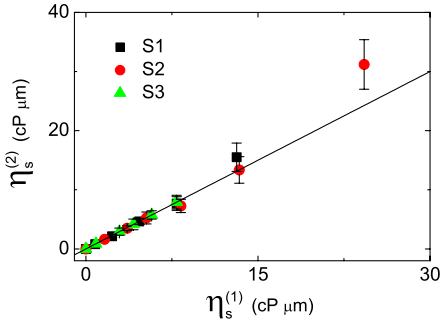

FIG. 3 (color online). Comparison between the obtained $\eta_s^{(2)}$ using Eq. (2) and $\eta_s^{(1)}$ for S1 (black squares), S2 (red circles), and S3 (green triangles). The solid line indicates $\eta_s^{(2)} = \eta_s^{(1)}$.

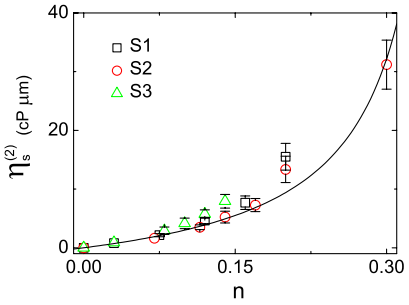

FIG. 4 (color online). Obtained $\eta_s^{(2)}$ using Eq. (2) as a function of n for S1 (black squares), S2 (red circles), and S3 (green triangles). The solid line is a fit of Eq. (3) to the red circles.

Figure 4 shows the obtained $\eta_s^{(2)}$ from Eq. (2) as a function of n for the three colloidal samples. All the data points with different particle sizes superpose onto a single curve. The solid line shows a fit using the Krieger-Dougherty equation [39],

$$\eta_s^{(2)}(n) = \eta_s^{(0)}\left[\left(1 - \frac{n}{n_m}\right)^{-[\eta]n_m} - 1\right], \tag{3}$$

where $\eta_s^{(0)} = \eta_b a k^{(0)}/k^{(1)}$ is the equivalent surface viscosity experienced by a single particle at the dilute limit, and $k^{(0)}$ is a known coefficient [38]. In the above, $n_m = 0.84(d/d^*)^2$ is the maximum area fraction of random packing, where $d^* = d + \lambda_D$ [33] with λ_D being the Debye screening length. For a hard sphere system, $d^* = d$ and one has $n_m \simeq 0.84$ [40,41]. The exponent $[\eta]$ (also called intrinsic viscosity) is the only fitting parameter. The data are well described by Eq. (3) (solid line) and the fitted values of $[\eta]$ are given in Table I.

Many analytical and numerical studies have been carried out to calculate $[\eta]$. The intrinsic viscosity for the hard disks (or spheres) in a 2D (or 3D) suspension is 2 (or $5/2$) at the dilute limit [42,43], and is $5/3$ for hard spheres half immersed at a liquid-liquid interface [44]. For 3D suspensions in the high concentration regime, a phenomenological model gives a value around 3.1 (or 2.7) under a low (or high) shear rate [45]. Table I reveals that the values of $[\eta]$ obtained in this experiment fall into the range of the calculated values of $[\eta]$. In addition, the obtained $[\eta]$ is found to depend on d [38].

The experiment clearly demonstrates that the correlated motion in the colloidal monolayers is well described by the normalized longitudinal and transverse diffusion coefficients, $\tilde{D}_\parallel(r/r_0) = D_\parallel/(k^{(1)}D_s')$ and $\tilde{D}_\perp(r/r_0) = D_\perp/(k^{(1)}D_s')$, where r_0 is a new scaling length characterizing the universal behavior of the correlated diffusion. These two universal functions are invariant with the particle size once the particle radius a is included in the definition of r_0 as shown in Eq. (2) [46]. The new scaling length r_0 can be understood in part by considering the squeeze force, $f_r = \xi_\parallel(r)U_r$, produced by an approaching sphere of radius a with velocity U_r toward another sphere at separation r. The two-particle friction coefficient $\xi_\parallel(r)$ is directly linked to the longitudinal diffusion coefficient via $D_\parallel(r) \simeq k_B T/\xi_\parallel(r)$ [25]. With the lubrication approximation for small r, one has $\xi_\parallel(\delta_{3D}) = (3/2)\pi\eta_b a(a/\delta_{3D})$, where δ_{3D} is the gap distance between the two spheres in the 3D flow [47]. Similarly, the squeeze force between two approaching circular disks of radius a in a thin film of thickness a and surface viscosity $\eta_s \simeq \eta_b a$ has the same expression with $\xi_\parallel(\delta_{2D}) = (3/2)\pi\eta_b a(a/\delta_{2D})^{3/2}$, where δ_{2D} is the gap distance between the two disks in the quasi-2D flow [48]. By equating the two squeeze forces [i.e., let $\xi_\parallel(\delta_{3D}) = \xi_\parallel(\delta_{2D})$], we find $\delta_{3D} = a(\delta_{2D}/a)^{3/2}$, which is the same equation as shown in Eq. (2).

This mapping of two-particle hydrodynamics in 3D to a 2D analogue thus provides an important insight into the observed universal scaling of correlated diffusion in colloidal monolayers. While the hydrodynamic interactions between the colloidal particles at the liquid interface are intrinsically 3D, the continuum hydrodynamic theory for molecular membranes can be extended to the colloidal monolayers, so long as the relevant scaling length r_0 in 3D is used to replace the corresponding 2D scaling length λ_S via Eq. (2). In this way, one can obtain the surface viscosity $\eta_s^{(2)}$ of the colloidal monolayers from r_0, and the results of two-particle rheology are found to agree well with those of one-particle rheology.

The discovery of the universal scaling functions $\tilde{D}_\parallel(r/r_0)$ and $\tilde{D}_\perp(r/r_0)$ reveals the relevant length involved in the many-body hydrodynamic interactions between the interfacial particles, which not only exchange momentum among themselves but also with the subphase liquid. The experiment provides a set of reliable data against which further theoretical modeling can be developed. It is also relevant to a class of problems related to the mobility and microrheology of interfacial particles in a monolayer or membrane, such as lipid or protein-associated domains in cell membranes [24–26].

We have benefited from useful discussions with Thomas Fischer, Jiangwei Zhang, Xiangjun Xing, and Jiang Xiao. This work was supported by the Hong Kong RGC under Grant No. HKUST-604310 (P. T.) and by the Bilateral Project BI-CN/11-13-013 (W. C. and K. B.).

*Corresponding author.
phchenwei@fudan.edu.cn

[1] B. P. Binks and T. Horozov, *Colloidal Particles at Liquid Interfaces* (Cambridge University Press, Cambridge, England, 2006).
[2] P. Pieranski, Phys. Rev. Lett. **45**, 569 (1980).
[3] N. D. Denkov, O. D. Velev, P. A. Kralchevsky, I. B. Ivanov, H. Yoshimura, and K. Nagayama, Nature (London) **361**, 26 (1993).

[4] J. R. Savage, D. W. Blair, A. J. Levine, R. A. Guyer, and A. D. Dinsmore, Science **314**, 795 (2006).

[5] Z. Zheng, F. Wang, and Y. Han, Phys. Rev. Lett. **107**, 065702 (2011).

[6] Z. Zhang, N. Xu, D. T. N. Chen, P. Yunker, A. M. Alsayed, K. B. Aptowicz, P. Habdas, A. J. Liu, S. R. Nagel, and A. G. Yodh, Nature (London) **459**, 230 (2009).

[7] F. Ghezzi and J. C. Earnshaw, J. Phys. Condens. Matter **9**, L517 (1997).

[8] J. Ruiz-Garcia, R. Gamez-Corrales, and B. I. Ivlev, Phys. Rev. E **58**, 660 (1998).

[9] W. Chen, S. S. Tan, T. K. Ng, W. T. Ford, and P. Tong, Phys. Rev. Lett. **95**, 218301 (2005).

[10] W. Chen, S. S. Tan, Z. S. Huang, T. K. Ng, W. T. Ford, and P. Tong, Phys. Rev. E **74**, 021406 (2006).

[11] Y. Peng, W. Chen, T. M. Fischer, D. A. Weitz, and P. Tong, J. Fluid Mech. **618**, 243 (2009).

[12] C. Y. Wu, Y. M Song, and L. L. Dai, Appl. Phys. Lett. **95**, 144104 (2009).

[13] R. Aveyard, B. P. Binks, and J. H. Clint, Adv. Colloid Interface Sci. **100–102**, 503 (2003).

[14] A. D. Dinsmore, M. F. Hsu, M. G. Nikolaides, M. Marquez, A. R. Bausch, and D. A. Weitz, Science **298**, 1006 (2002).

[15] E. M. Herzig, K. A. White, A. B. Schofield, W. C. K. Poon, and P. S. Clegg, Nat. Mater. **6**, 966 (2007).

[16] M Sickert, F Rondelez, and H. A Stone, Europhys. Lett. **79**, 66 005 (2007).

[17] V. Prasad, S. A. Koehler, and E. R. Weeks, Phys. Rev. Lett. **97**, 176001 (2006).

[18] M. H. Lee, S. P. Cardinali, D. H. Reich, K. J. Stebeb, and R. L. Leheny, Soft Matter **7**, 7635 (2011).

[19] Th. M. Fischer, P. Dhar, and P. Heinig, J. Fluid Mech. **558**, 451 (2006).

[20] J. C. Crocker, M. T. Valentine, E. R. Weeks, T. Gisler, P. D. Kaplan, A. G. Yodh, and D. A. Weitz, Phys. Rev. Lett. **85**, 888 (2000).

[21] A. J. Levine and T. C. Lubensky, Phys. Rev. Lett. **85**, 1774 (2000).

[22] A. J. Levine and F. C. MacKintosh, Phys. Rev. E **66**, 061606 (2002).

[23] P. G. Saffman, J. Fluid Mech. **73**, 593 (1976).

[24] P. G. Saffman and M. Delbruck, Proc. Natl. Acad. Sci. U.S.A. **72**, 3111 (1975).

[25] N. Oppenheimer and H. Diamant, Phys. Rev. E **82**, 041912 (2010); Biophys. J. **96**, 3041 (2009).

[26] Z. H. Nguyen, M. Atkinson, C. S. Park, J. Maclennan, M. Glaser, and N. Clark, Phys. Rev. Lett. **105**, 268304 (2010).

[27] C. Cheung, Y. H. Hwang, X-l. Wu, and H. J. Choi, Phys. Rev. Lett. **76**, 2531 (1996).

[28] B. Cui, H. Diamant, B. Lin, and S. A. Rice, Phys. Rev. Lett. **92**, 258301 (2004).

[29] E. R. Dufresne, T. M. Squires, M. P. Brenner, and D. G. Grier, Phys. Rev. Lett. **85**, 3317 (2000).

[30] H. A. Stone and A. Ajdari, J. Fluid Mech. **369**, 151 (1998).

[31] X. Qiu, X. L. Wu, J. Z. Xue, D. J. Pine, D. A. Weitz, and P. M. Chaikin, Phys. Rev. Lett. **65**, 516 (1990).

[32] P. Tong, X. Ye, and B. J. Ackerson, Phys. Rev. Lett. **79**, 2363 (1997).

[33] W. Chen and P. Tong, Europhys. Lett. **84**, 28 003 (2008).

[34] G. Tolnai, A. Agod, M. Kabai-Faix, A. L. Kovacs, J. J. Ramsden, and Z. Horvolgyi, J. Phys. Chem. B **107**, 11 109 (2003).

[35] See Supplemental Material at http://link.aps.org/supplemental/10.1103/PhysRevLett.111.168304 (Sec. I Experiment) for details.

[36] S. Ramachandran, S. Komura, and G. Gompper, Europhys. Lett. **89**, 56 001 (2010).

[37] P. P. Lele, J. W. Swan, J. F. Brady, N. J. Wagnera, and E. M. Furst, Soft Matter **7**, 6844 (2011).

[38] See Supplemental Material at http://link.aps.org/supplemental/10.1103/PhysRevLett.111.168304 (Sec. II Data Analysis) for details.

[39] I. M. Krieger and T. J. Dougherty, Trans. Soc. Rheol. **3**, 137 (1959).

[40] J. G. Berryman, Phys. Rev. A **27**, 1053 (1983).

[41] C. S. OHern, S. A. Langer, A. J. Liu, and S. R. Nagel, Phys. Rev. Lett. **88**, 075507 (2002).

[42] J. F. Brady, Int. J. Multiphase Flow **10**, 113 (1983).

[43] A. Einstein, Ann. Phys. (Berlin) **324**, 289 (1906).

[44] S. V. Lishchuk and I. Halliday, Phys. Rev. E **80**, 016306 (2009).

[45] A. J. Richard, *Soft Condensed Matter* (Oxford University Press, Oxford, England, 2002).

[46] We expect that this scaling is valid for interfacial particles with size in the range of 0.1–10 μm. See Supplemental Material at http://link.aps.org/supplemental/10.1103/PhysRevLett.111.168304 (Sec. II Data Analysis) for more details.

[47] W. B. Russel, D. A. Saville, and W. R. Schowalter, *Colloidal Dispersions* (Cambridge University Press, Cambridge, England, 1992).

[48] B. J. Hamrock, B. O. Jacobson, and S. R. Schmid, *Fundamentals of Fluid Film Lubrication* (Marcel Dekker, New York, 2004), 2nd ed.